POLİTEKNİK DERGİSİ

JOURNAL of POLYTECHNIC

ISSN: 1302-0900 (PRINT), ISSN: 2147-9429 (ONLINE)
URL: http://dergipark.org.tr/politeknik

Finite element simulation and experimental validation of welding distortion of fillet welded T-joints

T-Bağlantı kaynak deformasyonunun sonlu elemanlar yöntemi ile simülasyonu ve deneysel doğrulaması

***Yazar(lar) (Author(s))**: İlker EREN [1], Melike Sultan KARASU ASNAZ[2]*

ORCID[1]: 0000-0003-4326-0294

ORCID[2]: 0000-0003-4145-2524

Bu makaleye şu şekilde atıfta bulunabilirsiniz(To cite to this article): Eren İ. and Karasu Asnaz M.S., "Finite element simulation and experimental validation of welding distortion of fillet welded T-joints", ***Politeknik Dergisi***, 25(1): 455-466, (2022).

Erişim linki (To link to this article): http://dergipark.org.tr/politeknik/archive

DOI: **10.2339/politeknik.881438**

Finite Element Simulation and Experimental Validation of Welding Distortion of Fillet Welded T-Joints

Highlights

- *Computational modeling of distortion can minimize costly distortion corrections, and improve quality.*
- *The accuracy of this approach is highly dependent on the modeling of the heat source.*
- *The angular distortion found to be affected by welding speed, current, material thickness, penetration depth and pre-welding gap between plates. However, although it is said that there is a relationship between all inputs, there is no method to formulate how much they cause distortion.*
- *Quantifying the weld distortion is a challenging procedure. An adequate way to validate this type of study is to use precision measurement tools such as optical 3D scanner and coordinate measuring machine (CMM).*

Graphical Abstract

In this research, determination of welding parameters is carried out to improve the angular distortion and penetration depths in T-joints. Finite Element simulations and corresponding experiments are performed on S355J2G3 structural steel with thicknesses of 3mm, 5mm and 8mm, and finaly the results are compared and analyzed.

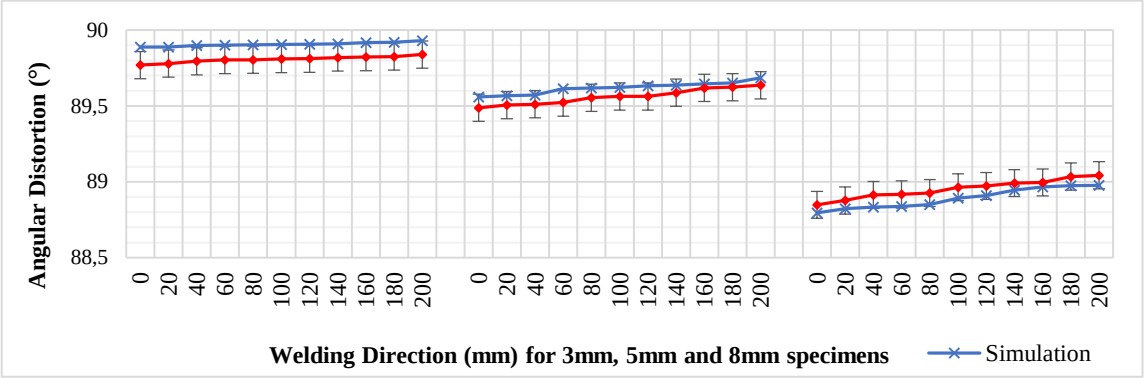

Figure. Angular distortion comparison of experimental and numerical results for all specimens (error amount is set to 0.1%)

Aim

The main goal of the research is to come up with a cost effective and a promising technique that will help to minimize the welding induced distortions and decrease costly design errors.

Design & Methodology

The non-linear heat transfer analysis is used and heat source is modeled with the Goldak's double ellipsoidal distribution by using SYSWELD in the gas metal arc welding.

Originality

The characteristics of the melt pool related to the material, and welding parameters were produced based on Goldak's semi-elllipsoidal heat input approach.

Findings

The agreement between the predicted results through FE simulation and the experimental study is generally good, and some amendments on heat source and welding parameters should be wisely done to reach better predictions.

Conclusion

Simulation is a very useful tool to estimate the welding parameters ahead of experiments, and it offers an economic and reliable solutions in order to prevent large costs that may occur after production by making the necessary changes during the design phase.

Declaration of Ethical Standards

The authors of this article declare that the materials and methods used in this study do not require ethical committee permission and/or legal-special permission.

Finite Element Simulation and Experimental Validation of Welding Distortion of Fillet Welded T-joints

Araştırma Makalesi / Research Article

İlker EREN[1*], Melike Sultan KARASU ASNAZ[2]

[1]Engineering Faculty, Department of Mechanical Engineering, Balıkesir University, Turkey
[2]Engineering Faculty, Department of Industrial Engineering, Balıkesir University, Turkey
(Geliş/Received : 16.02.2021 ; Kabul/Accepted : 15.03.2021 ; Erken Görünüm/Early View : 24.03.2021)

ABSTRACT

This research presents a numerical simulation for predicting welding induced distortion with an experimental validation. Three experimental specimens of S355J2G3 structural steel with thicknesses of 3mm, 5mm and 8mm have been used as test cases. In order to validate the results an experiment was set up to gain detailed information about distortions occurring in single fillet welded T-joints. The non-linear heat transfer analysis is used and heat source is modeled with the Goldak's double ellipsoidal distribution by using SYSWELD in the gas metal arc welding (GMAW) process. This study employs the finite element (FE) method to evaluate residual stresses and angular distortions. A series of FE simulations and corresponding experiments are performed to evaluate the depth of penetration in the cross sections, angular distortions that occur after welding, temperature distribution, and residual stresses. A coordinate measuring machine and a 3D non-contact scanning device are used to measure the angular distortions and displacement distributions, respectively. The results show that controlling welding process via simulations can significantly enhance the performance of process, and help to minimize distortions and decrease costly design errors.

Keywords: Welding distortion, residual stress, T-joint fillet weld, finite element model.

T-Bağlantı Kaynak Deformasyonunun Sonlu Elemanlar Yöntemi ile Simülasyonu ve Deneysel Doğrulaması

ÖZ

Bu araştırma, kaynak sebepli olabilecek distorsiyonları tahmin etmek için sayısal bir simülasyon ile bunun deneysel doğrulamasını sunmaktadır. 3mm, 5mm ve 8mm kalınlığındaki S355J2G3 yapı çeliğinden üç deneysel numune test edilmiştir. Simülasyon, SYSWELD programında yer alan gaz metal ark kaynağı (GMAW) ile tasarlanmış olup, ısı kaynağı Goldak'ın çift elipsoidal dağılımı ile modellenmiş ve hesaplamalarda doğrusal olmayan ısı transferi analizi kullanılmıştır. Sonuçları doğrulamak içinse tek köşe kaynaklı T-bağlantılarında meydana gelen bozulmaları analiz etmek üzere bir deney düzeneği kurulmuştur. Bu çalışmada, artık gerilmeleri ve açısal bozulmaları değerlendirmek için sonlu elemanlar (FE) yöntemi kullandı. Kesitlerdeki penetrasyon derinliğini, kaynak sonrası oluşan açısal bozulmaları, sıcaklık dağılımını ve artık gerilmeleri değerlendirmek için bir dizi FE simülasyonu ve ilgili deneyler gerçekleştirilmiştir. Deney sonuçları, kaynak işlemi henüz yapılmadan simülasyonlar yoluyla prosesin kontrol edilmesinin hem bozulmaları en aza indirmeye hem de maliyetli tasarım hatalarını azaltarak kaynak performansının artırılabileceğini göstermiştir.

Anahtar Kelimeler: Kaynak deformasyonu, artık gerilme, T-bağlantı kaynağı, sonlu elemanlar yöntemi.

1. INTRODUCTION

Welding is considered as one of the most reliable, practical and cost-effective technique to join metals permanently. Heating, melting, adding, solidification, and cooling treatments in the welding process cause inhomogeneous temperature distributions and material phase change in complex material structures. While inhomogeneous temperature distributions cause thermal expansion and contraction, the phase change which result in plastic deformations lead to both distortions and residual stresses [1]. Both situations have negative impacts on the manufacturing accuracy and desired properties of welded structures [2]. If the distortions can be accurately predicted in the design stage, it would benefit to achieve dimensionally capable and stable products. Since welding process is extensively used in the fabrication industry, the prediction of welding distortion has become a major concern in order to avoid modifications at great expenses. Trial and error approaches for the welding induced distortion and residual stress evaluation are inefficient and costly [3].

* *Corresponding Author*
e-mail : ieren@balikesir.edu.tr

Numerical, statistical, and empirical approaches are the three leading methods to estimate welding induced distortion. Numerical approach, which is the most commonly used by industry and academia [4], predicts the weld distortion by examining three categories which are transient analysis, shrinkage approach and local global analysis, as shown in Figure 1. Transient analysis is performed based on phase transformation and thermal material properties in order to simulate a better welding thermal history. The shrinkage approach is based on linear elastic analysis, and does not involve metallurgical analysis. And finally, the local global analysis predicts distortions for large parts by utilizing the transient analysis [5].

Welding simulations helps to optimize process parameters during the early stages of a new design avoiding expensive reworks that could occur later. The FE model has been used to investigate microstructure, predict distortion and residual stress due to welding process since 1980s [6]. Studies show that a great savings can be obtained by utilizing FE analysis that reduces downtime, machining requirements, and the capital for experimentation. With the aid of this analysis a planning tool is offered before the actual welding process itself and simultaneously with design [3].

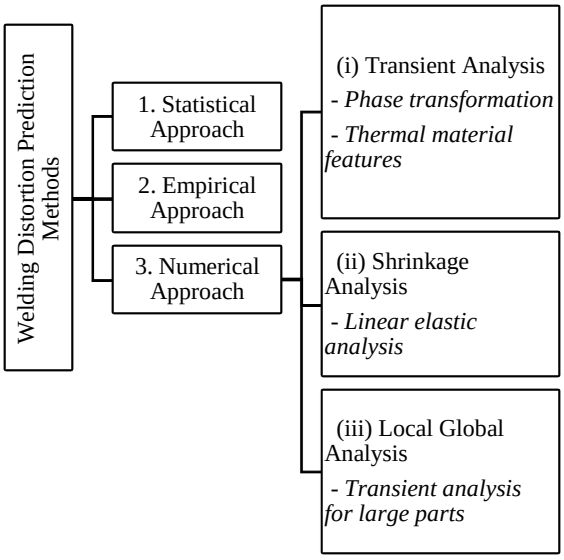

Figure 1. Welding distortion prediction methods

FE analysis of the welding procedure itself is a computer intensive approach. The most commonly used software and codes on welding are ABAQUS [7][8][9][10], ANSYS FE analysis [11][12], and SYSWELD[3] [4][13][14].

Mert et al. [15] studied the behavior of a double-fillet welded T-joint in terms of angular distortion, FE analysis was used for applying stress stretching on welds to eliminate weld shrinkage. Authors found out that lessen the temperature rise in the base metal reduced the penetration depth, which resulted in smaller angular distortion. Ramos et al. [3] investigated arc welding and laser beam welding (LBW) processes on a double side T-joint, and a T-joint between a steel tube and a plate. SYSWELD was utilized for FE analysis, and performed mesh sensitivity analysis in their study. It was concluded that hybrid meshes with tetrahedral and hexahedral elements are more efficient for small welding lengths.

In their study, Sun et al. [16] compared the welding distortion and residual stress processed by LBW and GMAW. It was concluded that residual stresses both in distribution and in magnitude, and distortions of thin-plate joint can be largely reduced in case of utilizing LBW. Mert et al. [15], and Manurung et al. [4] examined welding sequence effect on a multi-pass welding process, both research concluded that multi-pass welding resulted in greater distortion due to accumulation effects whereas single pass welding reduced distortion. Many studies investigated the effect of phase transformation on welding residual stress and distortions. Deng [10] examined this phenomena for low carbon (S15C) and medium carbon steels (S45C), and suggested that final residual stresses and distortions were highly influenced by phase transformation for medium carbon steels, while the influence was negligible for low carbon steel. Also, Zain-ul-abdein et al. [17] studied the same subject on an aluminum alloy AA 6056-T4 processed by LBW in a T-joint, found that the phase transformations has a slightly effect on welding distortions.

In this study, a series of FE simulations in SYSWELD and corresponding experiments are performed with low carbon S355J2G3 steel to evaluate angular distortion, residual stress and penetration depths due to GMAW processes on three different T-joints with thicknesses of 3mm, 5mm and 8mm plates. Heat source is modeled based on double-ellipsoid approach, and its shape parameters are determined after a couple of trial calculations. Numerical simulations and experimental tests are performed by using the adjusted parameters. The welded specimens are scanned with an optical scanning system after welding processes and the data are overlaid on 3D model. Thus, the degree of the distortions arising as a result of the welding process are determined, and compared with the numerical simulation in order to validate the model.

With this purpose, Section 2 of the study will explain the features of the experimental specimens; Section 3 explores the procedures of numerical simulation and theoretical background of distortion behavior due to welding; Section 4 discusses about the experimental study procedures; discussion and model validation examined; in Section 5 which the results of simulations and tests are presented; and finally conclusion is given in the last section.

2. MATERIAL and METHOD

2.1. Specimens

The process of single pass T-joints fillet welding of a base plate (200mm X 300mm) and a stiffener (200mm X

300mm) made of constructional steel S355J2G3 are used for the experiments. During this work, an attempt to predict the welding induced deformation on 3mm, 5mm and 8mm-thick plates used in heavy construction vehicle security cabins has been carried out.

S355J2G3 which widely used in the engineering industries is classified under high tensile strength and low carbon structural steel. The nominal chemical composition of S355J2G3 and the measured chemical composition which is obtained by arc atomic emission spectroscopy method used by SPECTRO xSORT are listed in Table 1. and, Table 2 shows the mechanical properties of S355J2G3.

Table 1. Nominal and measured chemical composition of the S355J2G3 steel

Elements (%)	EN 10025-2 / DIN17100 ST52-3	Specimen
Manganese (Mn)	max 1.60	0.93
Silicon (Si)	max 0.55	0.317
Chromium (Cr)	max 0.3	0.02
Nickel (Ni)	max 0.3	0.01
Carbon (C)	max 0.22	0.178
Molybdenum(Mo)	max 0.08	0
Phosphorus (P)	max 0.035	0.013
Sulfur (S)	max 0.035	0.005

Table 2. Mechanical Properties of S355J2G3 [18]

Elastic (Young's, Tensile) Modulus	**190 GPa**
Tensile Strength	355 MPa
Poissons`s ratio	0.29
Melting Completion (Liquidus)	1460 °C
Melting Onset (Solidus)	1420 °C
Thermal Diffusivity	13 mm^2/s
Specific Heat Capacity	470 J/kg-K
Impact Strength: V-Notched Charpy	28 J

In order to determine the base metal weldability, the carbon equivalent (CE) equations according to EN 1011-2 and American Welding Society (AWS) standards are used and these formulas are given in Eq.1 and Eq.2, respectively.

$$CE(\%) = C + \frac{Mn}{6} + \frac{Cr + Mo + V}{5} + \frac{Ni + Cu}{15} \quad (1)$$

$$CE(\%) = C + \frac{Mn}{6} + \frac{Si}{24} + \frac{Ni}{40} + \frac{Cr}{5} + \frac{Mo}{4} + \frac{V}{14} \quad (2)$$

The CE of the specimens was calculated prior to welding. The steels that have CE less than 0.45 % are considered as well weldable [19]. According to the formulas above, the CE values of the experimental specimens that are used in this study have 0.338 % and 0.350 % which support the conclusion that the steel has a good weldability property and the preheating prior to welding is not necessary.

GMAW which is widely used in the industry was chosen as the welding method, and a premixture of Ar / CO_2 (82% /18%) was used for executing the welding process. The procedure was executed in the horizontal position. With the help of a welding carriage, the torch angle was set to 45° for both the base plate and the stiffener as shown in Figure 2, and the angle was determined as 90°. A gas regulator was used to regulate the gas flow at the correct value.

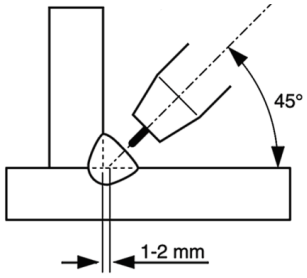

Figure 2. Torch angle and position across the welding direction at T-joint fillet welding [20]

3. NUMERICAL SIMULATION PROCEDURES

3.1. Finite element modelling

The reason of simulating a welding procedure with FE is to optimize the parameters [3]. FE analysis has been widely recognized and utilized in industry since it reflects comparable results with real life, and costs less compared to experiments [15].

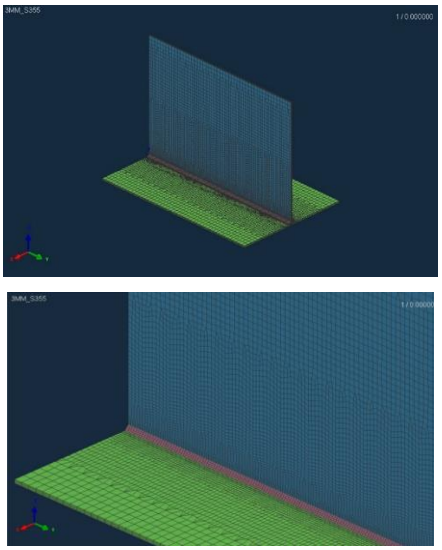

Figure 3. (a) Example of mesh analysis for the 200mm X 300mm X 3mm base plate and stiffener (b) Different mesh sizes

In this simulation, Quadratic mesh element in SYSWELD was chosen as the mesh element. The selected mesh element and size are two important factors for the results to reflect the accuracy of the values and the reliability of the results. Also, setting up mesh sizes is a way to reduce computational time since processing time significantly increases with increasing mesh size [3]. Smaller mesh size will provide more detailed examinations. Thus, the mesh size near the welding area was refined, so in the welding area and heat-affected zones it was determined as 1mm, while the farthest point of the plate where there is no welding was considered

7mm. The mesh analysis of the 3mm thick part is presented as an example in Figure 3 (a) and (b).

3.2. Thermal modelling

The thermal modelling takes an important place for an accurate prediction of the welding distortions [2]. The development of thermal modelling started in the 1940s by Rosenthal, and these studies gained speed in the 1980s thanks to powerful computer processors. The most favored heat source model in arc welding simulations is the double-ellipsoid model which was introduced in 1984 by Goldak. This heat source model includes two ellipsoidal heat sources which represents the front and the rear heat source [9]. Schematic of double ellipsoidal heat source model is shown in Figure 4. Goldak`s heat source equations in (x, y, z, t) coordinates are given below.

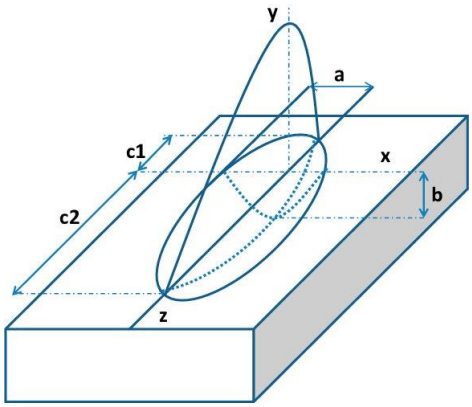

Figure 4. Double ellipsoidal heat source model [21]

$$q_f(x,y,z,t) = \frac{6\sqrt{3}Qf_f}{abc_1\pi\sqrt{\pi}} e^{-\left(\frac{3x^2}{a^2}+\frac{3y^2}{b^2}+\frac{3[z+v_w+(\tau+t)]}{c^2}\right)} \quad (3)$$

$$q_r(x,y,z,t) = \frac{6\sqrt{3}Qf_r}{abc_2\pi\sqrt{\pi}} e^{-\left(\frac{3x^2}{a^2}+\frac{3y^2}{b^2}+\frac{3[z+v_w+(\tau+t)]}{c^2}\right)} \quad (4)$$

$$f_f + f_r = \frac{2c_1}{c_1+c_2} + \frac{2c_2}{c_1+c_2} = 2 \quad (5)$$

$$Q = \eta IU \quad (6)$$

where q_f and q_r are the heat source on the front and the rear semi-ellipsoid in W/m^3, respectively. a, b, c_1 and c_2 are the heat source shape parameters; f_f represents the fraction of heat deposited in the front part of the heat source while f_r is the fraction of heat deposited at the back of the heat source, v_w is the welding speed in mm/min, t is the welding time, and τ is the offset distance in the welding direction. Q is the is the heat input that is transferred to the welding part, η is the arc efficiency; U and I are the welding voltage and current, respectively.

The Goldak`s heat source model as expressed in Eqs. 3 and 4 consist of seven ambiguous parameters: a, b, c_1, c_2, f_r, f_f, and η. According to [5], if the precise data does not exist, it is plausible to consider the distance in front of the heat source(c_1) is equal to half of the weld width(a), and the distance behind the heat source(c_2) is equal to two times of the weld width(a). Also, due to the continuity of the volumetric heat source the values for f_f and f_r are determined as $f_f + f_r = \frac{2c_1}{c_1+c_2} + \frac{2c_2}{c_1+c_2} = 2$ [22]. To simulate GMAW process, double ellipsoidal heat distribution is defined to SYSWELD program that offers FE methodologies.

Beside the heat source, heat losses due to convection and radiation are also considered in the FE analysis. A numerical procedure shown in Eq. 7 is applied to calculate the 3D heat transfer within the welding parts.

$$\frac{\partial}{\partial x}\left(k(T)\frac{\partial T}{\partial x}\right) + \frac{\partial}{\partial y}\left(k(T)\frac{\partial T}{\partial y}\right) + \frac{\partial}{\partial z}\left(k(T)\frac{\partial T}{\partial z}\right) + q_i = \rho c\left(\frac{\partial T}{\partial t} + v_w\frac{\partial T}{\partial y}\right) \quad (7)$$

Here, the weld is in the y direction, k is the thermal conductivity; T is the temperature; q_i represents internal heat generation; ρ is density; c is the specific heat capacity; v_w is the welding speed.

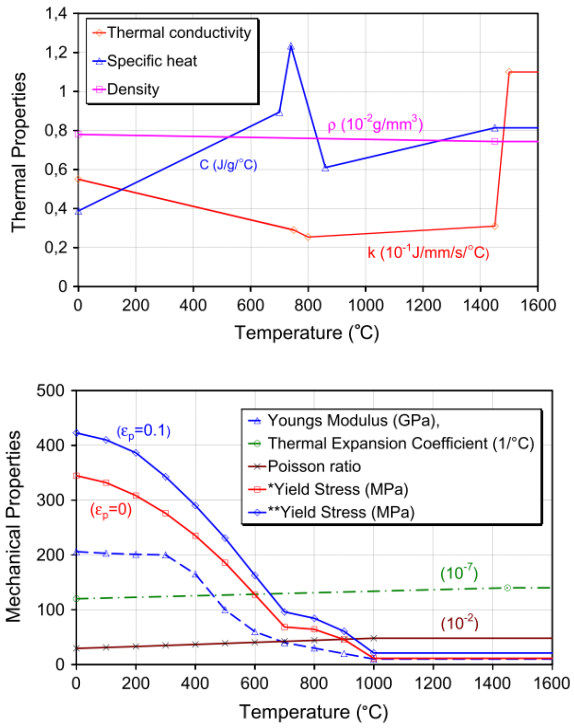

Figure 5. Variation of (a)Thermal properties and (b)Mechanical properties with the temperature for S355JR steel [23]

The thermal properties in Eq. 7 are all temperature dependent which needs consideration during welding. Thermal and mechanical properties variations are shown in the Figure 5 (a) and (b).

The effect of phase transformation on welding induced distortion was not considered in this study, since the phase transformations has a slightly effect on welding distortions in low-carbon materials according to the studies conducted by Deng [10] and Zain-ul-abdein et al. [17].

3.3. Numerical simulation results

In SYSWELD a 3D model based on FE analysis has been developed accounting for the thermal and the mechanical properties of the workpieces. The Welding Simulation Solution tool under this program runs the solver and manages the computation of the distortions of the experimental specimens. To execute the simulation, all the input data required by the program is provided and the results are explained further in this section. Also, Metallurgical Parameters Fitting tool makes available to fit the metallurgical parameters of phase transformations during the welding process.

The predicted data used for this study are based on the applications of the case study company, and compliant with the Goldak's double ellipsoid explained aforementioned. To determine the heat source parameters, the size and shape of the melt pool of a previously welded part was measured. Accordingly, initial values were given for each parameter. By using these values, the profile of the melt pool was created by a trial calculation in SYSWELD. By comparing the results, the value of each parameter was adjusted until a reasonable melt pool was obtained similar to the experimental result in both shape and size. After a couple of trial calculations and adjustments, the final heat source and welding parameters were determined and summarized in Table 3.

Welding distortions are the consequences of the non-uniform temperature fields emerging during the welding process. The rapid heating and cooling of the welding process lead to uneven thermal expansions and contractions on the stiffener and the base plates, where different shrinkage forces warp these plates. The temperature distribution along the stiffener and the base plate causes fillet weld angular distortions [1].

Figure 6 shows the results of the temperature profile and the angular distortion simulation for 3mm thick specimen. The angle between the two plates, which was 90° at the beginning, are estimated to be 89.904° for 3mm, 89.597° for 5mm and 88.904° for 8mm. According to this simulation, only 0.1%, 0.4% and 1.2% of angular changes due to welding has occurred. As suggested by [24] and seen in the results of this study, thicker structures, 8mm in this case, cause to higher angular distortions because of the higher thickness thermal gradients.

One of the major causes of geometrical error in the welding process are the initial gaps and misalignments of the welded structures [25]. In another study [26] by the same authors, it is suggested that the amount of gap and misalignment have the same effect as inherent deformation due to welding. The initial gap values determined as 0.5mm, 1mm and 1mm decreased to 0.176mm, 0.479mm and 0.316mm, respectively, according to the numerical study.

Table 3 Welding parameters for each experimental workpiece

	3mm specimen	**5mm specimen**	**8mm specimen**
Weld width ($\boldsymbol{a}$)	6 mm	6 mm	7 mm
Weld depth ($\boldsymbol{b}$)	3 mm	3 mm	3 mm
Front weld length ($\boldsymbol{c_1}$)	3 mm	3 mm	3.5 mm
Rear weld length ($\boldsymbol{c_2}$)	12 mm	12 mm	14 mm
Voltage ($\boldsymbol{U}$)	22 V	22 V	30 V
Current ($\boldsymbol{I}$)	170 A	170 A	200 A
Arc efficiency ($\boldsymbol{\eta}$)		0.70	
Welding speed ($\boldsymbol{v_w}$)	450 mm/min	450 mm/min	280 mm/min
Gap between base and stiffener	0.5 mm	1 mm	1 mm
Welding Position	Fillet weld in PB / 2F position		
Shielding Gas	Premixture of Ar - CO_2 (82% - 18%)		
Thermal conductivity ($\boldsymbol{k}$)	49 W/m-K		
Density ($\boldsymbol{\rho}$)	7.8 g/cm^3		
Specific heat capacity ($\boldsymbol{c}$)	470 J/kg-K		

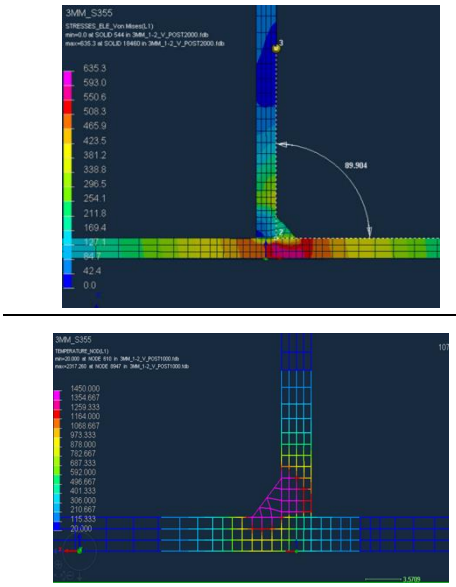

Figure 6. Angular distortion and temperature profile for 3mm thick specimen

The visualized results obtained from the analysis in form of residual stress and welding penetration depths are presented in Figure 7. High residual stresses in regions near the weld areas which may promote brittle fracture, fatigue, or stress corrosion cracking [27] are clearly seen in the left side of Figure 7. The residual stresses and the penetration depths of all three welded specimens are measured at the beginning, the midpoint and the end.

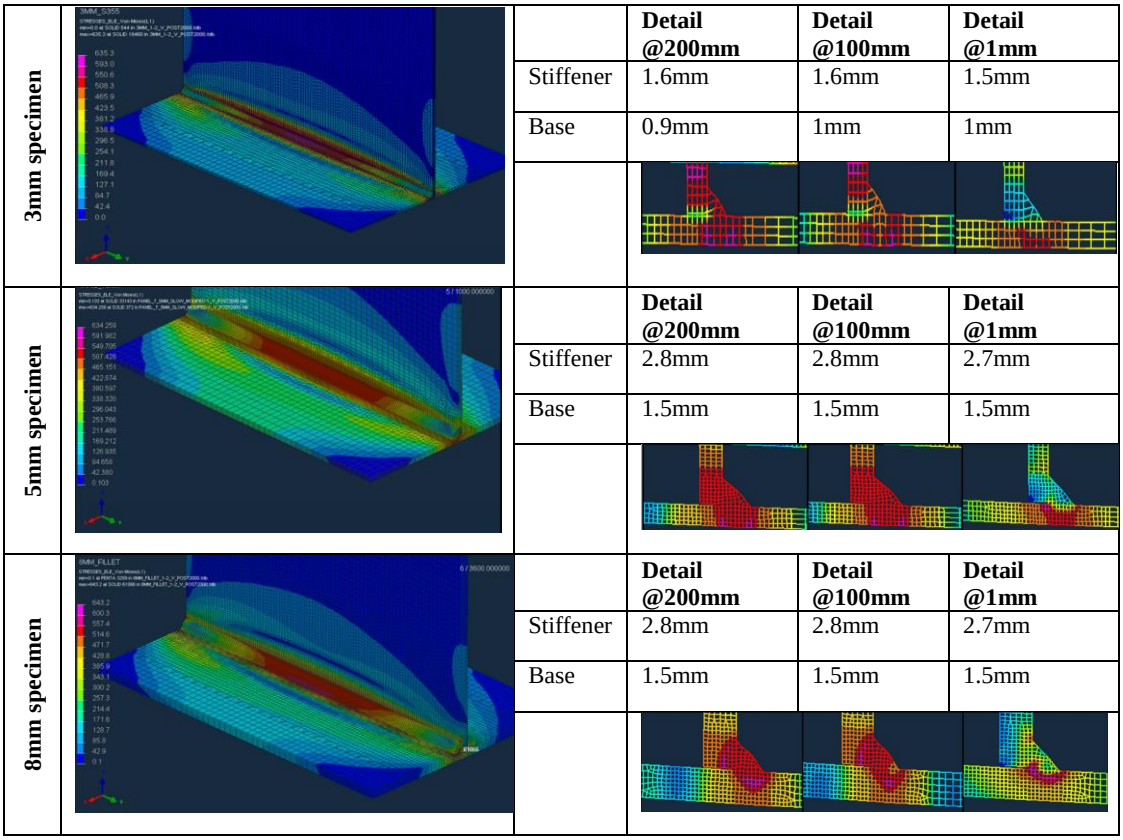

	Detail @200mm	Detail @100mm	Detail @1mm
Stiffener	1.6mm	1.6mm	1.5mm
Base	0.9mm	1mm	1mm

	Detail @200mm	Detail @100mm	Detail @1mm
Stiffener	2.8mm	2.8mm	2.7mm
Base	1.5mm	1.5mm	1.5mm

	Detail @200mm	Detail @100mm	Detail @1mm
Stiffener	2.8mm	2.8mm	2.7mm
Base	1.5mm	1.5mm	1.5mm

Figure 7. Residual stress and detailed views of welding penetration depths for all specimens

Detailed views and simulation results for both the base and the stiffener plates are presented on the right side of Figure 7. It was assumed that the material is followed the Von Mises Stress criterion.

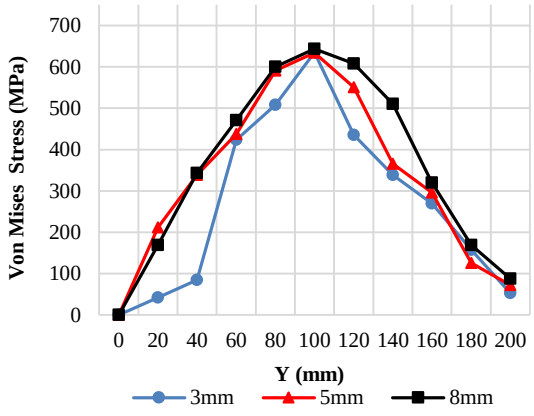

Figure 8. Von Mises Stress distribution for 3mm, 5mm and 8mm thickness specimens

According to simulation, a high tensile stress is produced near the welded area for all specimens, and the areas far from the weld bead showed low stress. Also, the lowest stress values are observed at the edges of each plates for all specimens while the highest stress are at the midpoint of the joints. The distribution of Von Mises stress along the weld bead for each specimen is given in Figure 8.

According to the research [7], thicker plates increase the residual stresses, in correlation with the results of this simulation.

4. EXPERIMENTAL STUDY PROCEDURES

In order to validate the results an experiment was set up to gain detailed information about distortions occurring in three different fillet welded T-joints. The parameters used for this study are based on the applications of the case study company, and presented above in Table 3. After completing the welding process, the displacement measurements and angular distortions were measured, and finally penetration depths were analyzed by examining macro elements.

4.1. Pre-welding Measurements

Before the welding process, four holes were drilled in the base plates to be used as a reference for measurements to be made after the process. The flatness of all test specimens was checked with a portable coordinate measuring machine (CMM) as shown in Figure 9 (a). A CMM has a sensitive electronic probe to measure a series of discrete points from the geometry of a solid part, and provides reliable measurements of complex shapes and surfaces [28]. After ensuring the flatness of the parts do not have any deformation that will affect the welding process, the stiffener was tacked down to the base plate in order to keep these two parts fixed during the welding

process, seen in Figure 9 (b). After the tack welding process, the angle between the two plates was controlled by CMM, as seen in Figure 9 (c). This angle must be within a 0.02° tolerance, so the slope of the stiffener was set to be within this range. In this study, Leica T-Probe as the CMM was employed for both flatness and angular measurement control. Finally, an edge preparation was made on the T-joint where the two plates were positioned 90° each other. Two small pieces were tacked to the both endings of the specimens using GTAW in order to eliminate welding defects associated with starting and stopping welding. When the process was done these two pieces were intently cut out.

4.2. Post-Welding Measurements

A single pass T-joint fillet welding was executed for all the specimens of different thicknesses. A summary of the process parameters used throughout this study are shown in Table 3. The non-uniform temperature distribution during welding causes residual stresses and deformation. Thus, a result of non-uniform expansion and contraction due to the local heating and follow up cooling causes volumetric changes called distortions[1].

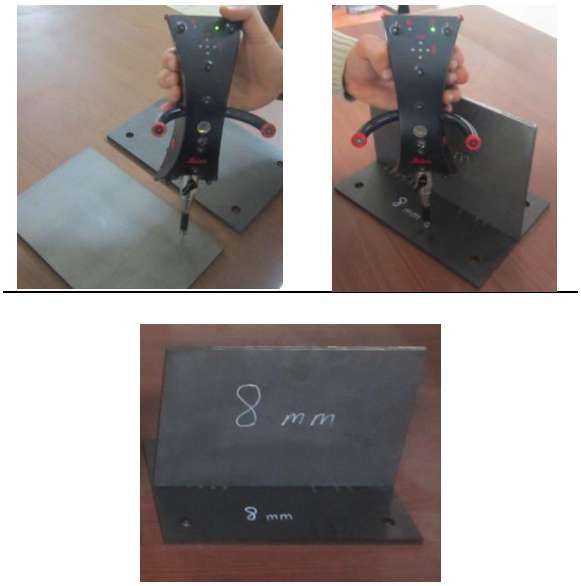

Figure 9. (a) Flatness measurement of 8 mm thick specimen by Leica T-Probe (b) Tack weld process to hold the parts in the proper location (c) Angular control of two parts by Leica T-Probe

The welding-induced distortion was experimentally investigated using an optical 3D scanner that collects a detailed and high resolution point cloud that could be analyzed without needing further additional manipulation[1]. Shown in Figure 10 (a), GOM ATOS Core which operates with narrowband blue LED light was used to determine the angular distortion and displacement measurements. The advantage of using this machine in distortion measurements is that it can produce precise measurements regardless of ambient light conditions as it uses blue LED light.

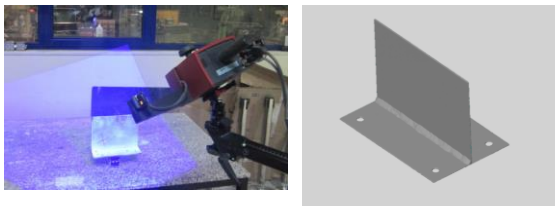

Figure 10. (a) Image of the welded part during 3D scanning, (b) Scanned Image of the welded part

The angular distortions were observed along the length of the joint with little variations. The angle between the base plate and the stiffener, which was 90º before welding, was measured after the welding process. The method used for angular distortion measurement is scanning the welded part with the GOM device, seen in Figure 10 (a), after 20 s of weldment cooling. The data obtained by GOM is consists of a cloud of points, seen in Figure 10 (b). This cloud was transformed into mesh and then compared with the model by examining the angle between the planes.

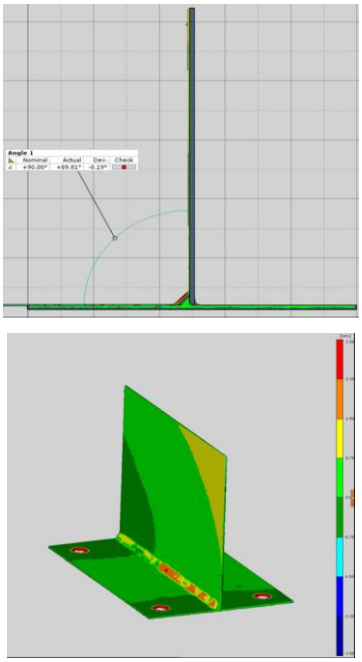

Figure 11. (a) Examination of angular distortion (b) Color distribution of displacement

The proportion of welding induced angular distortion can be seen more clearly when the scanning data is overlapped with the actual model as in Figure 11 (a). According to the color distribution in Figure 11 (b), the extent of the displacements after welding can be seen.

5. DISCUSSION AND MODEL VALIDATION

The cooling process of welded parts that are heated up to the melting temperature locally is slower than the heating process. For this reason, the temperature distribution in the welded part is not uniform during the cooling process

which causes structural and metallurgical changes along the joint. Due to localized heating by the welding process and subsequent rapid cooling, residual stresses and distortions can occur near the T-joint [27].

Measurements with GOM along the weld bead was recorded, and the maximum values of angular distortion results are provided in Table 4. As can be easily seen in this table, a very good agreement has been achieved between experiments and simulations in terms of angular distortions. According to [1], the angular distortions are affected by the thickness of steel, welding speed and level of penetration.

Table 5 shows the maximum distortion value among the weld bead, and the relative differences between simulation and experiment results. Penetration depth measurements were taken along the weld bead in both numerical and experimental studies, and it was observed that there was no significant difference. For the calculations of error amount and rates, maximum data in simulation and experiment were taken into account. According to the results of this study, the deepest penetration weld (2.615mm) and the largest prediction error rate (10.18%) appears in the 5mm specimen.

There are three main factors affecting weld penetration depth: current, welding speed, and type of shielding gas. Current is the most directly variable of all which affects penetration depth. As the current increases in the welding process the penetration increases meaning a better quality and more fully fused weld [1]. The second factor determining penetration is the welding speed. As the welding speed increases, the penetration decreases, because the duration of the arc over a certain point decrease. The last factor is the protective or shielding gas. Shielding gas types with high thermal conductivity such as 100% CO_2 or 100% Ar have deeper penetration characteristics. A shallower penetration is observed in shielding gas with low thermal conductivity such as 100% Ar, Ar/CO_2 or Ar/O_2. In this study, current and welding speed were examined, but the shielding gas was not taken into account in terms of penetration depth since it was the same for all three specimens.

Current and welding speed are the two main welding parameters that influence the extent of distortion. Increasing the current up to a certain level causes an increase in distortion. However, as increased current provides deeper penetration which improves angular distortion, then increased current may lead to a reduction in overall distortion. For this reason, the current and welding speed should be considered together and adjusted in a harmony, and efforts should be made to reach an optimal heat input.

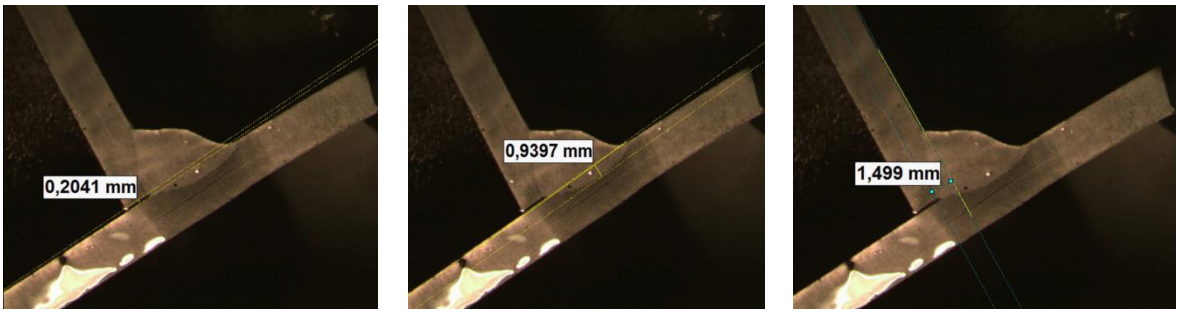

Figure 12. Example of macro sections of the welded specimen to examine the weld gap and penetration depts for both plates

Table 4. Comparison the result of angular distortion in degrees

	3mm specimen	5mm specimen	8mm specimen
Simulation	89.904	89.597	88.904
Experiment	89.81	89.56	88.96
Error	0.094	0.037	0.056
Error %	0.10%	0.04%	0.06%

By comparing the results of all three specimens, the angular distortion errors are between 0.10% and 0.04%, which is an acceptable range for the case study company. When comparing 3mm and 5mm specimens with same current, voltage and welding speeds, it is observed that the 5mm specimen performs better results in both numerical simulation and experimental study with 0.04% error ratio. There are two reasons behind such a result. In the studies of [25] and [29], the authors proved that lower welding speed will lead the high angular distortion. With respect to this research, it is concluded that the welding speed determined for the 3mm specimen which was 450mm/min was not fast enough for a piece of such thickness. However, in the case of increasing the speed of welding, the heat input will be insufficient that would cause a shallow penetration. So, increasing welding speed should be supported with the current increment in order to keep the optimal heat input. The other reason is found to be the gap between the two plates is insufficient corresponds to an increase in distortion. The graph showing the variation of the experimental and numerical results of the angular changes after welding along the joint are presented in Figure 13.

Table 5. Comparison of the average result of penetration depths in mm

	3 mm specimen		5 mm specimen		8 mm specimen	
values in mm	**Base**	**Stiffener**	**Base**	**Stiffener**	**Base**	**Stiffener**
Simulation *(range)*	0.9 - 1.0	1.5 - 1.6	1.5	2.7 - 2.8	1.0- 1.1	1.0 - 1.2
Simulation *(max)*	1.00	1.600	1.500	2.800	1.100	1.200
Experiment	0.94	1.499	1.670	2.615	1.181	1.155
Error	0.06	0.101	0.170	0.185	0.081	0.045
Error %	6.42 %	6.74 %	10.18 %	7.07 %	6.86 %	3.90 %

In the experiment, current and weld speeds were the same for 3mm and 5mm specimens, and penetration depths at the base and stiffener were (0.940, 1.499) and (1.670, 2.615), respectively. The reason for a deeper penetration in the 5mm specimen is the generated heat input was ideal such a thick part, and using the same current and welding speed values for a thinner material did not produce optimal results.

The purpose of the case study company is to achieve deep penetration depths in their welding processes. So, either increasing current or increasing welding speed for 3mm specimen would result in reduced in distortion. However, higher heat input leads a consistent and deeper penetration, so increasing current up to a certain point in this case would be wisely, because heat input is inversely proportional to the welding speed and directly proportional to the current.

The penetration depth found for the 8mm specimen was not deep enough for the company. Simulation produced a maximum of 1.1mm depth for the base plate and 1.2mm for the stiffener, while in actual welding process they were reached up to 1.181mm and 1.155mm. As the company claimed that angular distortion is more tolerable than penetration depth for their welded parts, it can be suggested that the current should be adjusted to more than 200A for a higher heat input. Also, considering the thickness of this specimen, heat source shape parameters can be determined by another approach in order to reach a deeper and tolerable penetration depth.

Table 6. Comparison of the average result of weld gap in mm	**3mm specimen**	**5mm specimen**	**8mm specimen**
Pre-welding gap	0.5	1	1
Simulation	0.1676	0.479	0.316
Experiment	0.2044	0.446	0.416
Error	0.0283	0.033	0.100
Error %	13.77%	7.40 %	23.97%

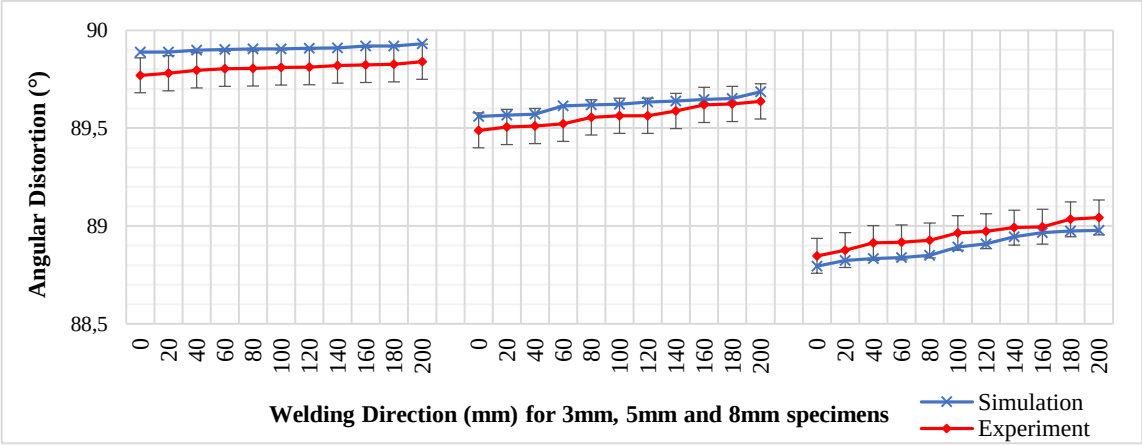

Figure 13. Angular distortion comparison of experimental and numerical results for all specimens (error amount is set to 0.1%)

Another possible improvement was considered to see whether the distortion might be related to the welding gap. According to Deng et al. [25], initial weld gaps have significant influence on the final welding distortion. Under the conditions of the company, clamping or fixturing was not possible[1], hence the plates were tacked to avoid movement during welding.

Large welding gaps can increase the extent of distortion as it will increase the amount of weld metal required to fill the gap. Based on the results presented in Table 6, the range of error between the simulation and the experiment results for all experiments is between 0.028mm and 0.1mm, which draws a satisfactory prediction. However, since the penetration depth of the 8mm specimen was not satisfactory for the company, increasing the weld gap by a certain degree can be considered besides the solutions offered above.

In this study, firstly the welding parameters were determined, and then numerical and experimental studies were made according to these parameters. The maximum prediction error rates are found as follows; 0.10% for angular distortion, 10.18% for penetration depth, and 23.97% for the weld gap. The distortion predictions from the simulation and the experiment results were satisfactory for the case study company. In brief, the agreement between the predicted results through FE simulation and the experimental study is generally good, and some amendments on heat source and welding parameters should be wisely done to reach better predictions.

Future Studies

It has been realized that obtaining reliable results depends entirely on parameter determination. Additional efforts should be made to evaluate for the procedure of parameters determination by employing design of experiments, artificial neural networks or meta-heuristic optimization methods. In addition, the scarcity of studies on the financial impact due to weld distortions in welding industries has drawn attention. Both authors of this study agree that the subject will be more noticeable for the industry if the studies on welding distortion predictions are presented together with the economic consequences.

6. CONCLUSION

The research focuses on the GMAW model of three T-joints with different thicknesses. Numerical approach is followed to predict the welding induced distortions, then experimental study is performed in order to validate the results. The following conclusions can be drawn according to the numerical and experimental study explained in detail in the previous chapters,

- Multiple considerations causing to residual stresses and distortions like thermal, metallurgical and mechanical shifts should be taken into consideration during welding process. Computational modeling of distortion can minimize costly distortion corrections, and improve quality.
- One of the main difficulties in this research was to quantify the weld distortion. Accurate measurement of the pre- and post-welding parts is particularly important for the validation of numerical and experimental study. By this study, it can be said that an adequate way to obtain sufficient results is to use precision measurement tools such as optical 3D scanner and CMM.
- The simulations were solved with SYSWELD. The computational time for each simulation was about an hour for the transient analysis. It is found that SYSWELD is a very useful tool to estimate the welding parameters ahead of experiments, and it offers an economic and reliable solutions in order to avoid expensive welding distortions. Therefore, SYSWELD has a great potential to determine the distortions in advance for more complicated welded parts in a short computational time.
- The accuracy of this approach used in this study is highly dependent on the modeling of the heat source. In order to obtain reliable predictions, the shape and the size formed along the joint should be well analyzed while determining the parameters. Therefore, it will be very helpful to make trial calculations before determining the parameters precisely.

DECLARATION OF ETHICAL STANDARDS

The author(s) of this article declare that the materials and methods used in this study do not require ethical committee permission and/or legal-special permission.

AUTHORS' CONTRIBUTIONS

İlker EREN: Conceived and designed the analysis. Performed the analytic calculations and performed the numerical simulations.

Melike Sultan KARASU ASNAZ: Contributed data, performed the analysis, wrote the manuscript.

CONFLICTS OF INTEREST

The authors declare no conflict of interest.

REFERENCES

[1] R.W. O'Brien, "Predicting weld distortion in the design of automotive components," MSc thesis, School of Engineering, Durham University, Durham, United Kingdom, 2007, [Online]. Available: http://etheses.dur.ac.uk/2462 [Accessed: 10-Sep-2020].

[2] Y. Li, K. Wang, Y. Jin, M. Xu, and H. Lu, "Prediction of welding deformation in stiffened structure by introducing thermo-mechanical interface element," ***Journal of Materials Processing Technology***, 216:440–446, (2015).

[3] H. M. E. Ramos, S. M. O. Tavares, and P. M. S. T. de Castro, "Numerical modelling of welded T-joint configurations using SYSWELD," ***Science and Technology of Materials***, 30: 6–15, (2018).

[4] Y. H. P. Manurung *et al.*, "Welding distortion analysis of multipass joint combination with different sequences using 3D FEM and experiment," ***International Journal of Pressure Vessels and Piping***, 111: 89–98, (2013).

[5] F. Folchi, "Weld Distortion Prediction With Virtual Analysis For Practical Weld Distortion Prediction With Virtual Analysis For Practical Applications Applications," MSc thesis, Department of Mechanical, Automotive and Material Engineering, University of Windsor, Windsor, Ontario, Canada, 2014. [Online]. Available: https://scholar.uwindsor.ca/etd/5229 [Accessed: 3-Sep-2020].

[6] P. Michaleris and A. Debiccari, "Prediction of welding distortion," ***Welding Journal (Miami, Fla)***, 76(12): 172-181, (1997).

[7] M. J. Attarha and I. Sattari-Far, "Study on welding temperature distribution in thin welded plates through experimental measurements and finite element simulation," ***Journal of Materials Processing Technology***, 211(4): 688–694, (2011).

[8] D. F. Fu, C. Q. Zhou, C. Li, G. Wang, and L. X. Li, "Effect of welding sequence on residual stress in thin-walled octagonal pipe-plate structure," ***Transactions of Nonferrous Metals Society of China (English Edition),*** 24(3): 657–664, (2014).

[9] D. Klobčar, J. Tušek, and B. Taljat, "Finite element modeling of GTA weld surfacing applied to hot-work tooling," ***Computational Materials Science***, 31(3): 368–378, (2004).

[10] D. Deng, "FEM prediction of welding residual stress and distortion in carbon steel considering phase transformation effects," ***Computational Materials Science***, 30(2): 359–366, (2009).

[11] K. Venkateswarlu, P. N. Kumar, and P. S. Ravikumar, "Finite Element Simulation of Temperature Distribution , Distortion and Residual Stresses of Dissimilar Welded Joints," ***Materials Today: Proceedings***, 5(5):11933–11940, (2018).

[12] I. Sattari-Far and Y. Javadi, "Influence of welding sequence on welding distortions in pipes," ***International Journal of Pressure Vessels and Piping***, 85(4):265–274, (2008).

[13] J. Rahman, M. Vasudevan, S. Muthukumaran, and R. R. Kumar, "Simulation of laser butt welding of AISI 316L stainless steel sheet using various heat sources and experimental validation," ***Journal of Materials Processing Technology***, 219: 48–59, (2015).

[14] C. Heinze, C. Schwenk, and M. Rethmeier, "Influences of mesh density and transformation behavior on the result quality of numerical calculation of welding induced distortion," ***Simulation Modelling Practice and Theory,*** 19(9):1847–1859, (2011).

[15] T. Mert, C. L. Tsai, S. S. Babu, and Y. P. Yang, "Strain-based assessment and modeling for low-distortion welding procedure," ***Materials and Manufacturing Processes***, 27(9): 943–948, (2012).

[16] J. Sun, X. Liu, Y. Tong, and D. Deng, "A comparative study on welding temperature fields, residual stress distributions and deformations induced by laser beam welding and CO2 gas arc welding," ***Materials and Design***, 63: 519–530, (2014).

[17] M. Zain-ul-abdein, D. Nélias, J. F. Jullien, F. Boitout, L. Dischert, and X. Noe, "Finite element analysis of metallurgical phase transformations in AA 6056-T4 and their effects upon the residual stress and distortion states of a laser welded T-joint," ***International Journal of Pressure Vessels and Piping***, 88(1): 45–56, (2011).

[18] "Material Properties EN 1.0570 (S355J2G3) Non-Alloy Steel." [Online]. Available: https://www.makeitfrom.com/material-properties/EN-1.0570-S355J2G3-Non-Alloy-Steel. [Accessed: 14-Jul-2020].

[19] V. Lazić *et al.*, "Qualification of the welding technology of the structural steel S355J2G3," ***IOP Conference Series: Materials Science and Engineering***, Prague, 419:1-12, (2018).

[20] K. Weman, "MIG/MAG welding," ***Welding Processes Handbook***, 75–97, (2012).

[21] J. Bai, R. D. Goodridge, S. Yuan, K. Zhou, C. K. Chua, and J. Wei, "Thermal influence of CNT on the polyamide 12 nanocomposite for selective laser sintering," ***Molecules***, 20(10): 19041–19050, (2015).

[22] N. T. Nguyen, Y. W. Mai, and A. Ohta, "Analytical solution for a new hybrid double-ellipsoidal heat source in semi-infinite body," ***Proceedings of International Conference on Advances in Composite Materials and Structures VII,*** Bologna, 207–217, (2000).

[23] M. Perić *et al.*, "Numerical analysis and experimental investigation of welding residual stresses and distortions in a T-joint fillet weld," ***Materials and Design***, 53:1052–1063, (2014).

[24] D. Deng and H. Murakawa, "FEM prediction of buckling distortion induced by welding in thin plate panel structures," ***Computational Materials Science***, 43(4): 591–607, (2008).

[25] D. Deng, H. Murakawa, and W. Liang, "Numerical simulation of welding distortion in large structures," ***Computer Methods in Applied Mechanics and Engineering***, 196: 4613–4627, (2007).

[26] H. . Murakawa, D. . Deng, S. Rashed, and S. . Shinji, "Prediction of Distortion Produced on Welded Structures during Assembly Using Inherent Deformation and Interface Element," ***Transactions***

of Japan Welding Research Institute., 38(2): 63–69, (2009).

[27] T. L. Teng, C. P. Fung, P. H. Chang, and W. C. Yang, "Analysis of residual stresses and distortions in T-joint fillet welds," ***International Journal of Pressure Vessels and Piping***, 78(8): 523–538, (2001).

[28] "HEXAGON - Manufacturing Intelligence Division." [Online]. Available: https://www.hexagonmi.com/. [Accessed: 16-Sep-2020].

[29] G. Fu, M. I. Lourenco, M. Duan, and S. F. Estefen, "Effect of boundary conditions on residual stress and distortion in T-joint welds," ***Journal of Constructional Steel Research***, 102:121–135, (2014).